Support Information

High output characteristic Ag_2Se/Nylon self-supporting composite films for wearable photo-thermoelectrical generators

Zhen-yu Yang,[§a] Xin-zheng Jin,[§a] Wen-yan Wang,[a] Chen-hui Huang,[a] Yan-zhou Lei,[b] Yong Wang*[a]

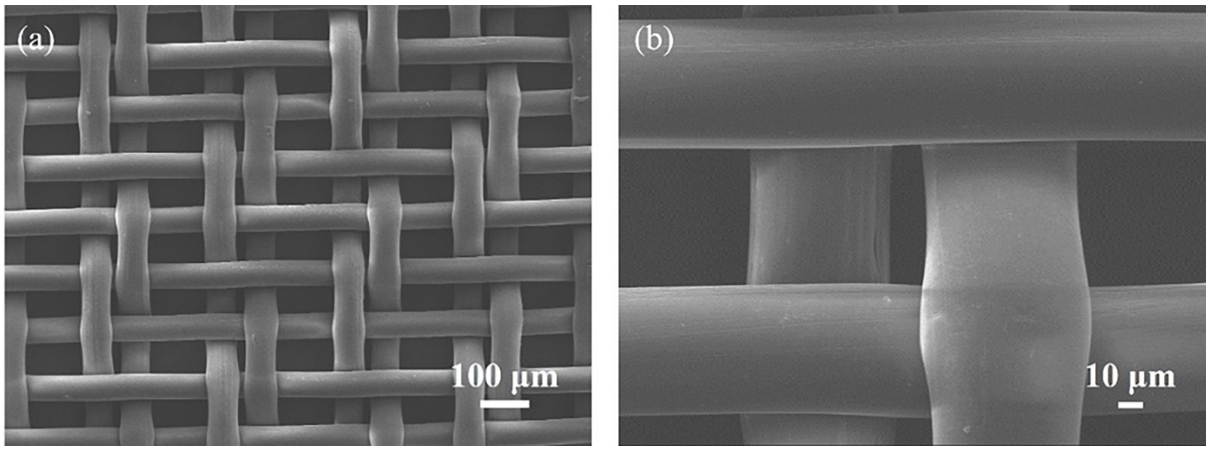

Figure S1. (a) Low and (b) high magnification surface FESEM images of commercial nylon mesh.

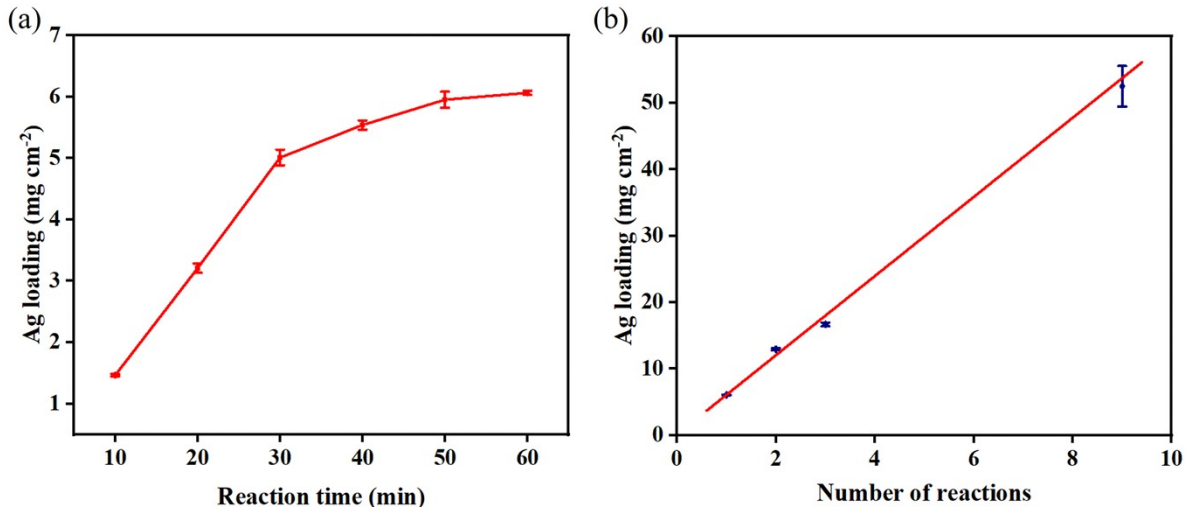

[a] School of Materials Science & Engineering, Key Laboratory of Advanced Technologies of Materials (Ministry of Education), Southwest Jiaotong University, Chengdu 610031, China. Phone: +86 28 87603042; Email: yongwang1976@swjtu.edu.cn

[b] Analytical and Testing Center, Southwest Jiaotong University, Chengdu 610031, China

[§] Co-first author. **ORCID:** Yong Wang: 0000-0003-0655-7507

Figure S2. Variation of silver loading in the silver mirror reaction with (a) reaction time and (b) numbers.

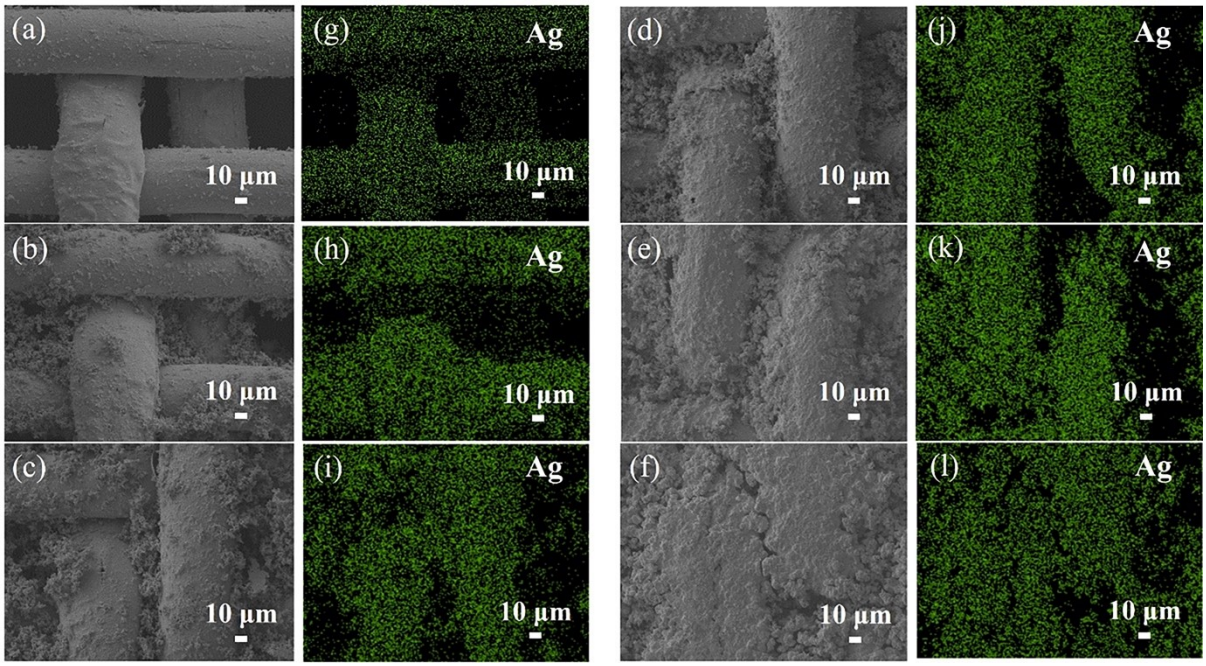

Figure S3. The morphologies of (a) 15Ag/85Nylon, (b) 35Ag/65Nylon, (c) 50Ag/50Nylon, (d) 60Ag/40Nylon, (e) 75Ag/25Nylon and (f) 90Ag/10Nylon. The EDS patterns of (g) 15Ag/85Nylon, (h) 35Ag/65Nylon, (i) 50Ag/50Nylon, (j) 60Ag/40Nylon, (k) 75Ag/25Nylon and (l) 90Ag/10Nylon.

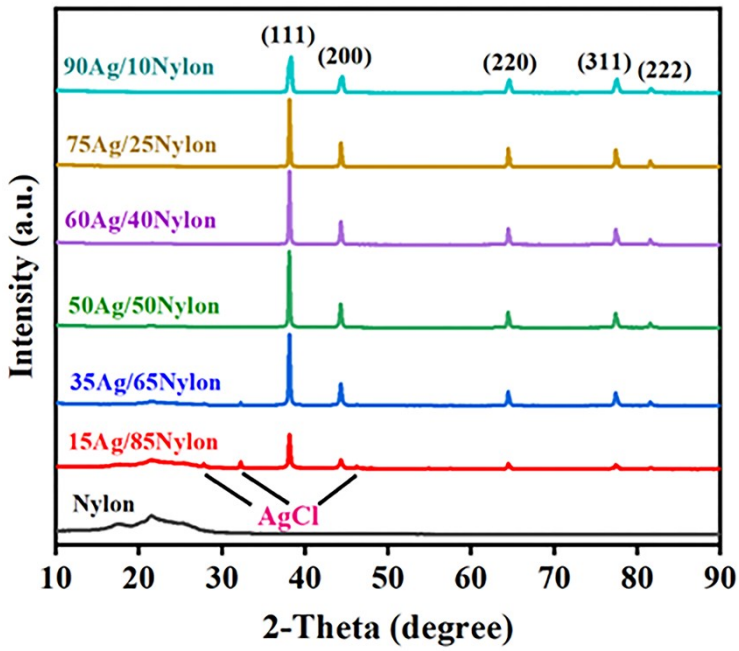

Figure S4. The XRD patterns of the nylon mesh and the prepared Ag/Nylon composite films with different contents of sliver.

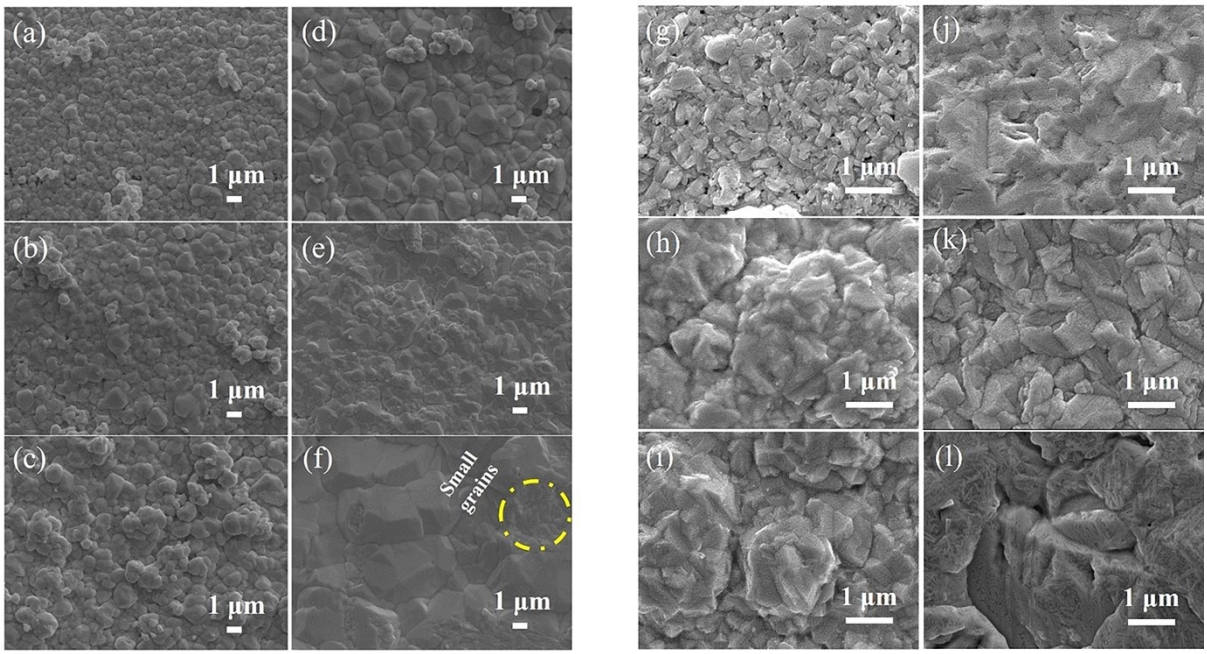

Figure S5. High magnification surface FESEM images of (a) 15Ag/85Nylon, (b) 35Ag/65Nylon, (c) 50Ag/50Nylon, (d) 60Ag/40Nylon, (e) 75Ag/25Nylon, (f) 90Ag/10Nylon, (g) $20Ag_2Se/80$Nylon, (h) $40Ag_2Se/60$Nylon, (i) $60Ag_2Se/40$Nylon, (j) $70Ag_2Se/30$Nylon, (k) $80Ag_2Se/20$Nylon and (l) $90Ag_2Se/10$Nylon.

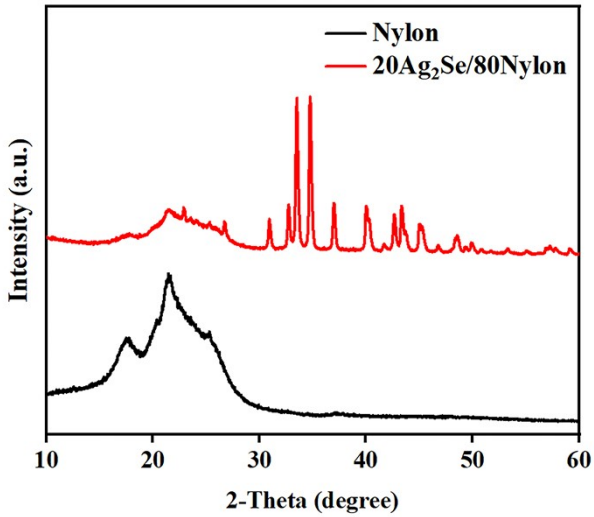

Figure S6. The XRD patterns of the nylon mesh and the prepared $20Ag_2Se/80$Nylon composite film.

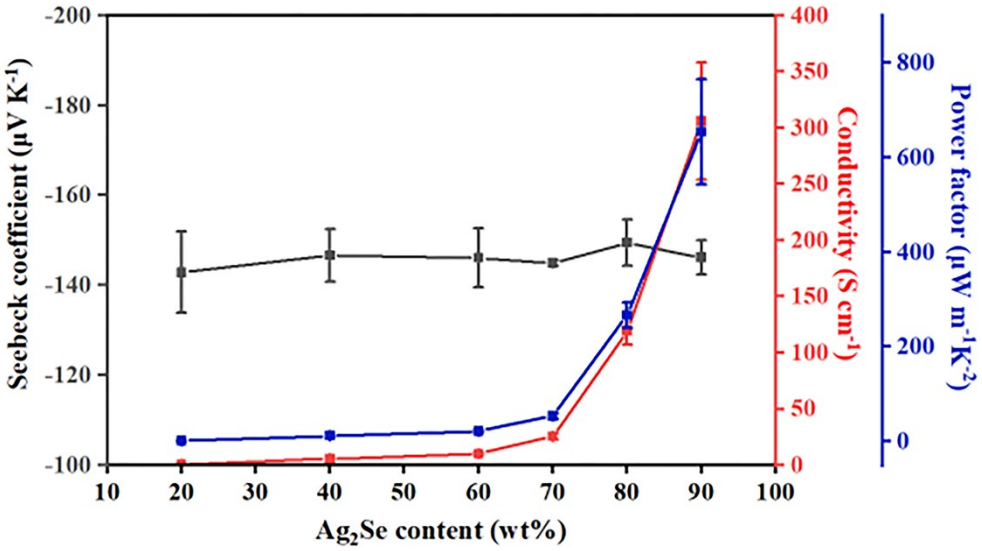

Figure S7. The electrical conductivity, Seebeck coefficient and power factor of Ag_2Se/Nylon composite films with different loadings.

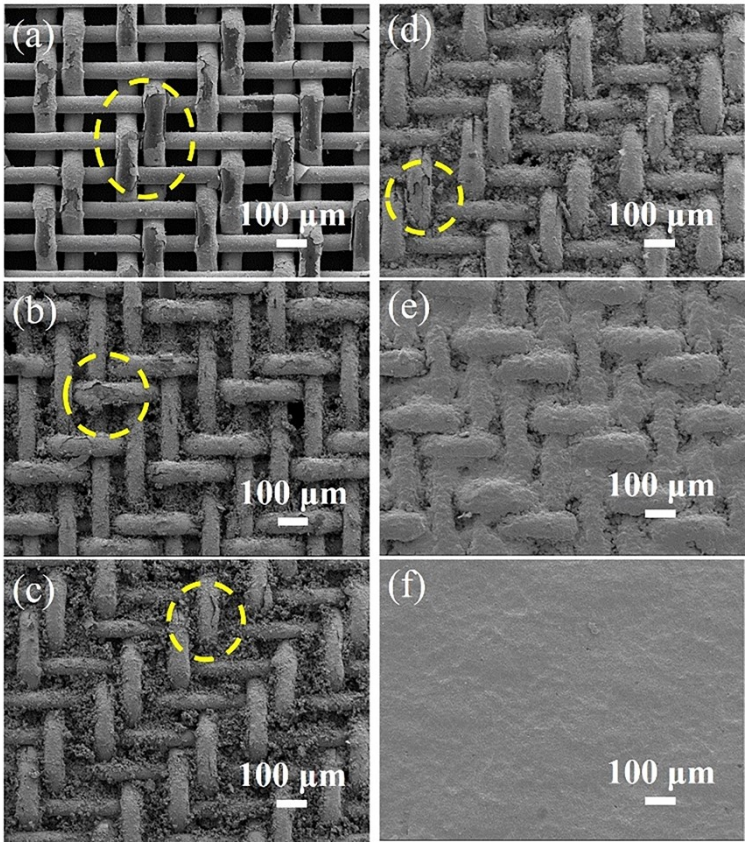

Figure S8. Low magnification surface FESEM images of (a) 20Ag_2Se/80Nylon, (b) 40Ag_2Se/60Nylon, (c) 60Ag_2Se/40Nylon, (d) 70Ag_2Se/30Nylon, (e) 80Ag_2Se/20Nylon and (f) 90Ag_2Se/10Nylon. Where the place marked by the yellow dotted line occurs obvious shedding phenomenon, the thicker Ag_2Se layers present in the higher content samples make the shedding of a small amount of Ag_2Se not lead to bare leakage, so the obvious

shedding phenomenon is not easily observed.

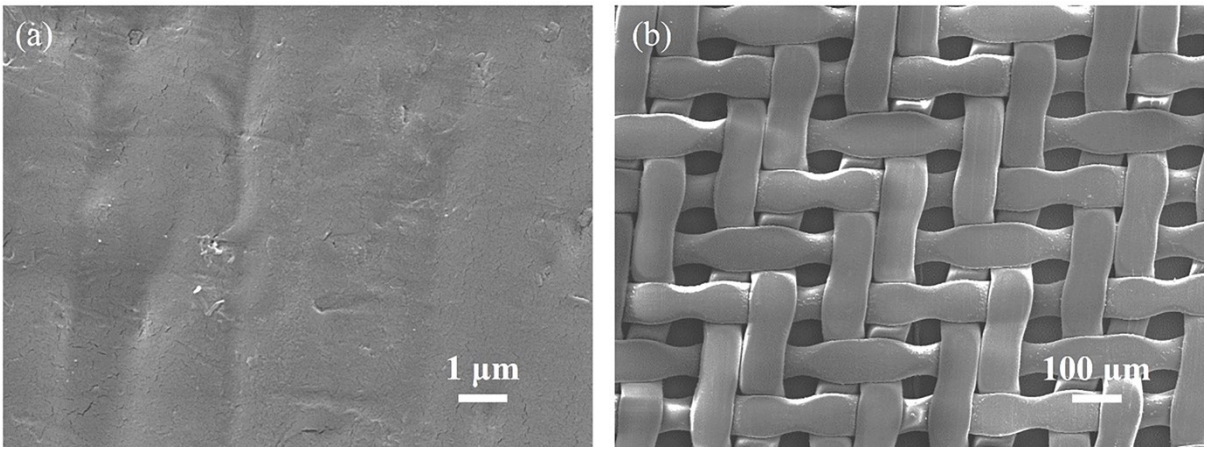

Figure S9. (a) High and (b) low magnification surface morphologies of nylon mesh after hot-pressing.

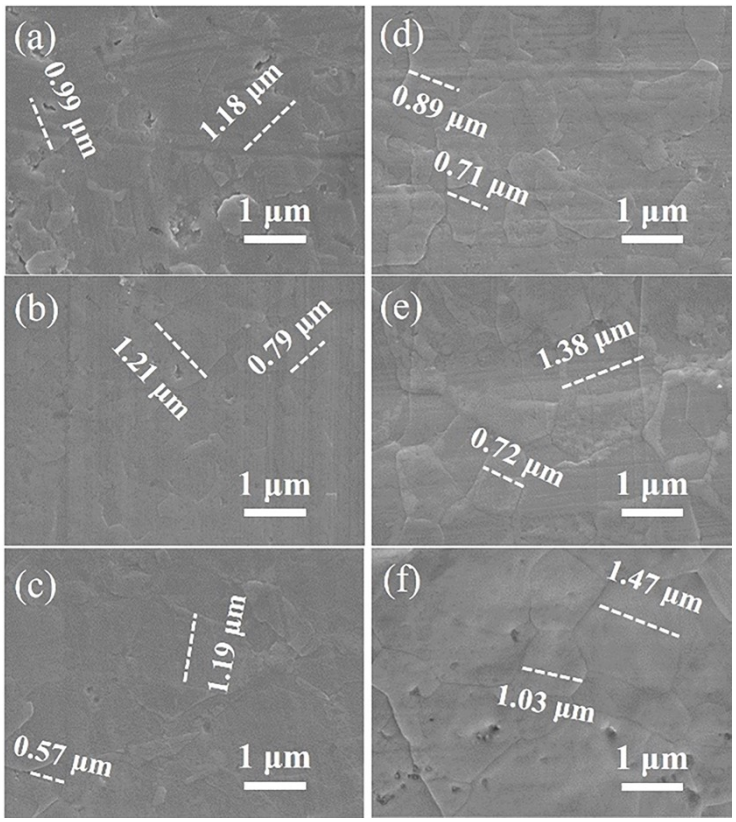

Figure S10. The morphologies of Ag_2Se grains in Ag_2Se/Nylon composite films after hot pressing. Figures a-f show 20Ag_2Se/80Nylon-h, 40Ag_2Se/60Nylon-h, 60Ag_2Se/40Nylon-h, 70Ag_2Se/30Nylon-h, 80Ag_2Se/20Nylon-h and 90Ag_2Se/10Nylon-h in order.

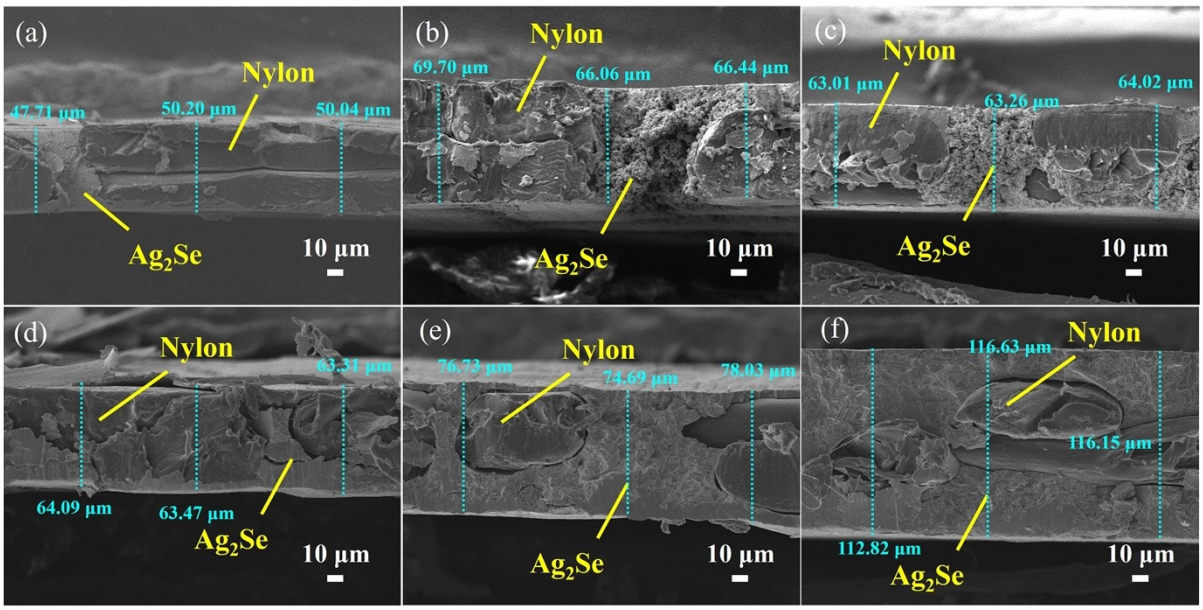

Figure S11. The cross-sectional FESEM images of Ag_2Se/Nylon composite films after hot pressing. Figures a-f also show composite films with Ag_2Se contents of (a) 20wt%, (b) 40wt%, (c) 60wt%, (d) 70wt%, (e) 80wt% and (f) 90wt%.

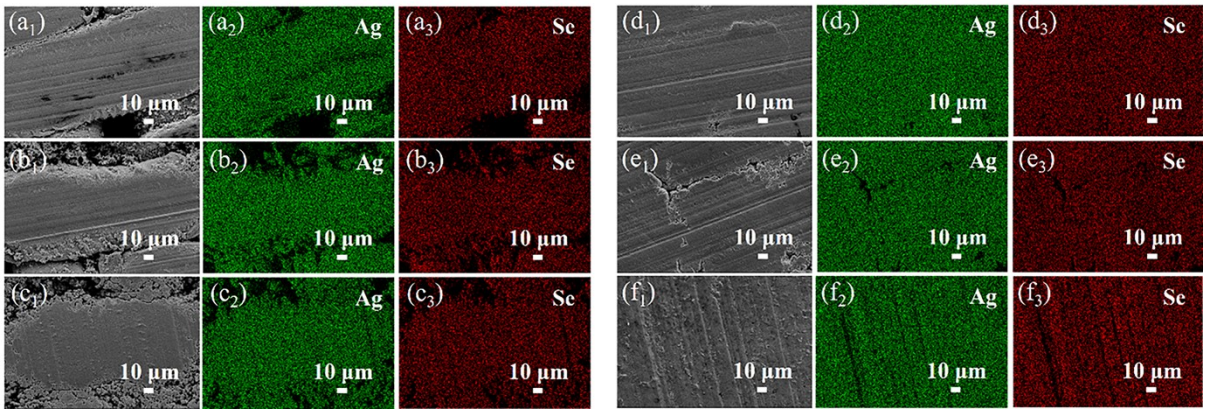

Figure S12. The EDS patterns of (a) $20Ag_2Se$/80Nylon-h, (b) $40Ag_2Se$/60Nylon-h, (c) $60Ag_2Se$/40Nylon-h, (d) $70Ag_2Se$/30Nylon-h, (e) $80Ag_2Se$/20Nylon-h and (f) $90Ag_2Se$/10Nylon-h.

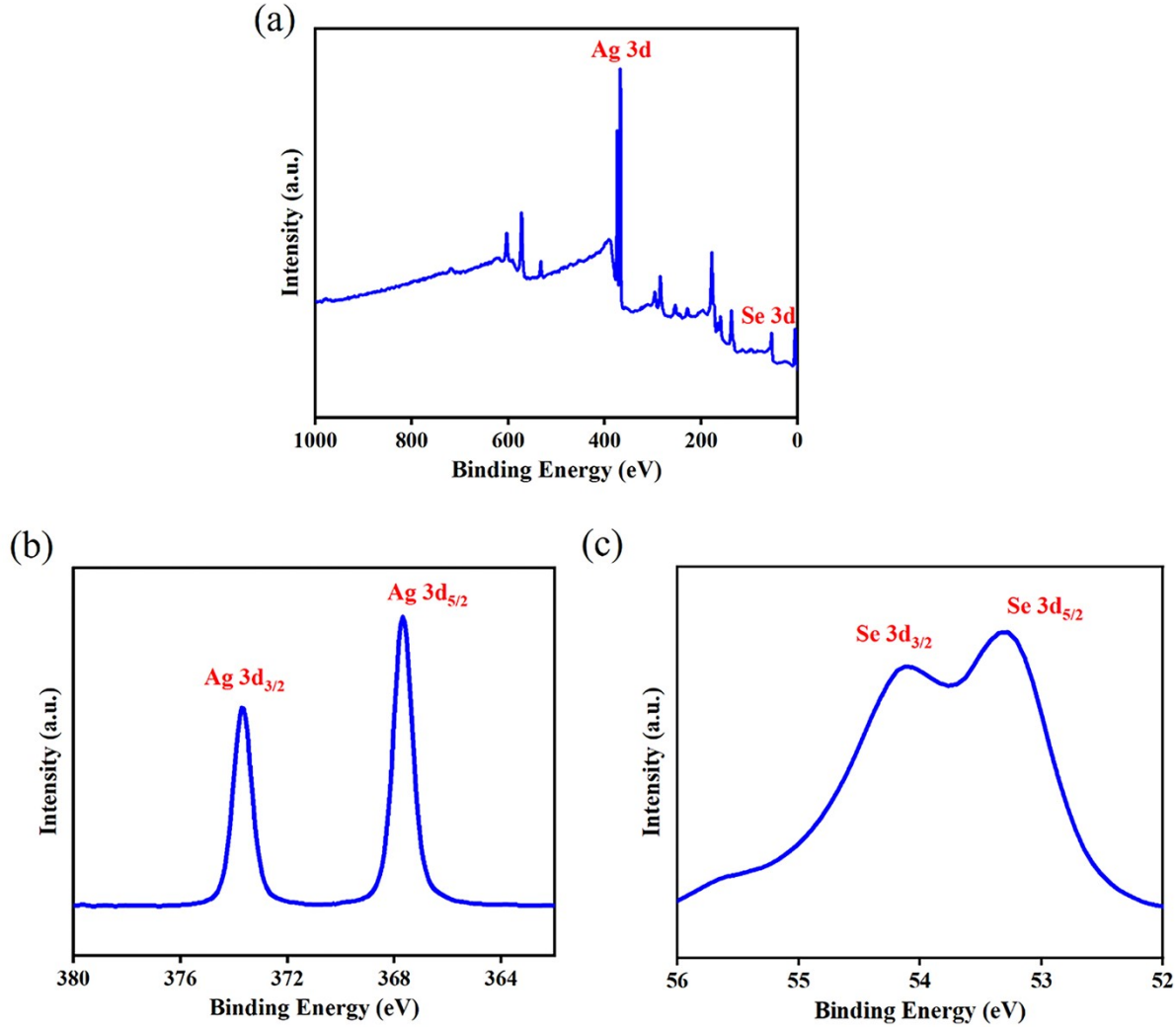

Figure S13. (a) XPS survey spectrum, and high-resolution Ag 3d (b) and Se 3d (c) core level spectra of the 80Ag_2Se/20Nylon-h.

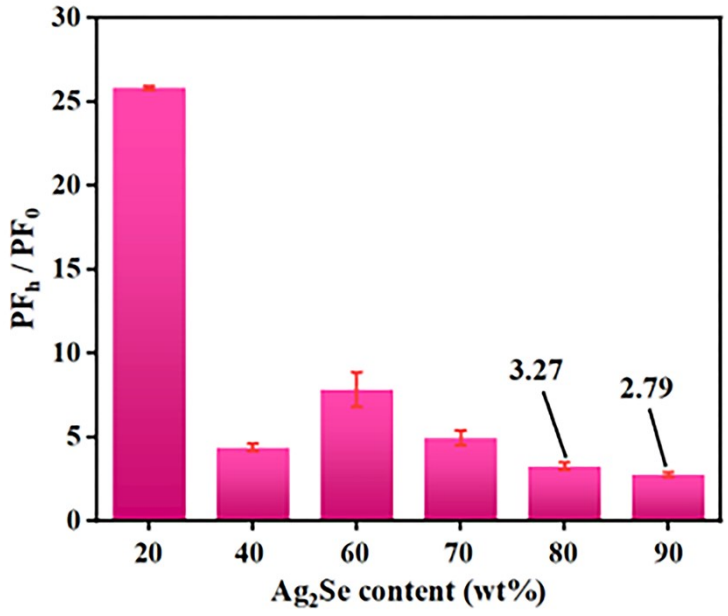

Figure S14. The ratio of the power factor of the composite films after hot-pressing to the composites before hot-pressing. PF_0 and PF_h are the power factors of the Ag_2Se/Nylon composite film before and after hot-pressing respectively.

Tables S1. The density, specific heat capacity, out-of-plane and in-plane thermal diffusivity of the $xAg_2Se/yNylon$-h composite films obtained from the measurements.

Sample	Density ($g\ cm^{-3}$)	Specific heat capacity ($J\ g^{-1}\ K^{-1}$)	Out-of-plane thermal diffusivity (mm^2s^{-1})	In-plane thermal diffusivity (mm^2s^{-1})
$20Ag_2Se/80Nylon$-h	1.36	1.048	0.130±0.008	0.538±0.007
$40Ag_2Se/60Nylon$-h	1.61	0.930	0.129±0.030	0.545±0.014
$60Ag_2Se/40Nylon$-h	1.83	0.834	0.131±0.005	0.538±0.010
$70Ag_2Se/30Nylon$-h	2.50	0.627	0.133±0.017	0.545±0.026
$80Ag_2Se/20Nylon$-h	3.41	0.458	0.135±0.001	0.534±0.007
$90Ag_2Se/10Nylon$-h	4.93	0.317	0.168±0.001	0.519±0.003

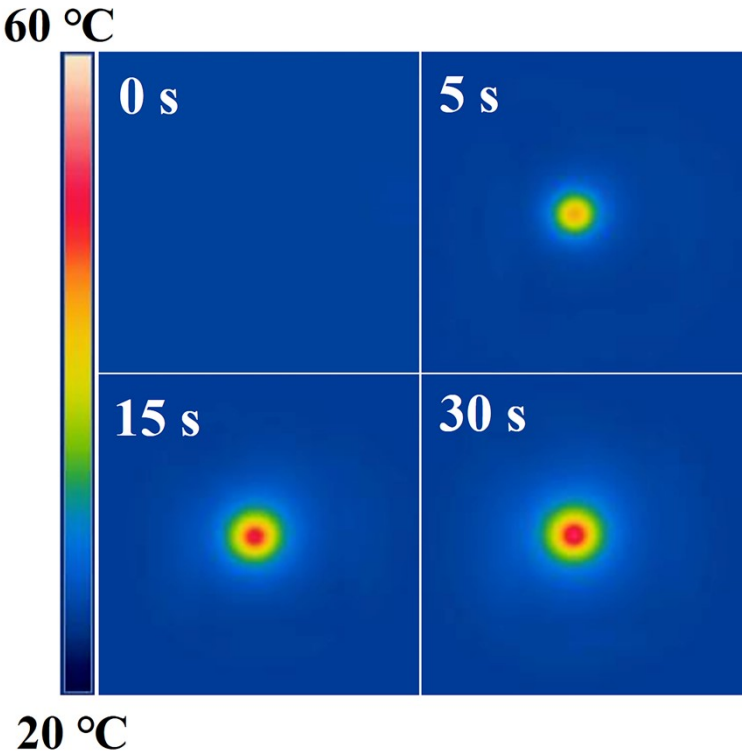

Figure S15. IR heat maps of the $80Ag_2Se/20Nylon$-h when irradiated by 180 mW cm^{-2} NIR light. The recording time of heat maps is 0 s, 5 s, 15 s and 30 s respectively.

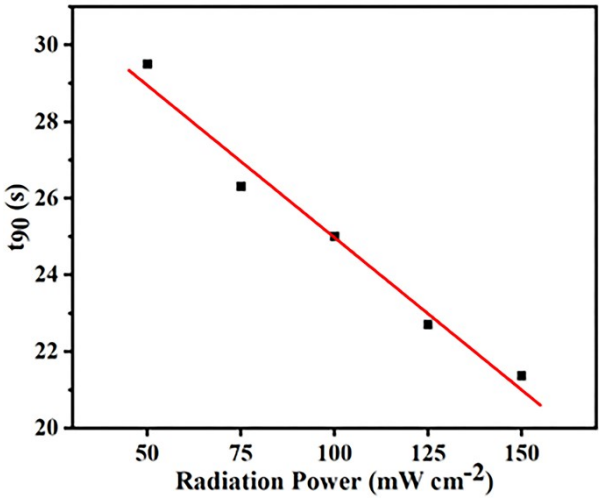

Figure S16. The time required for the PTEG to reach 90% of the maximum open-circuit output voltage with different power light radiation.

Tables S2. Comparison of our work with the reported power densities of PTEGs with different types.

Index	Composite	Light source mode	The number of legs	Power densities (nW cm^{-2})	Ref
1	$Bi_2Te_{2.7}Se_{0.3}/Sb_2Te_3$	20 mW cm^{-2} (NIR, 808 nm)	10	502.78	1
2	PPy/Ag_2Se	100 mW cm^{-2} (NIR, 808 nm)	1	600.00	2
3	PEDOT:PSS/HCNTs	166.01 mW cm^{-2} (NIR, 808 nm)	3	2.83	3
4	PPy/HCNTs	400 mW cm^{-2} (NIR, 808 nm)	1	0.0446	4
5	Mo_2S/PU-PEDOT:PSS/Te NWs	2625 mW cm^{-2} (NIR, 808 nm)	1	0.0432	5
6	**Ag_2Se/Nylon**	**100 mW cm^{-2} (NIR, 808 nm)**	**4**	**3265.63**	**Our work**

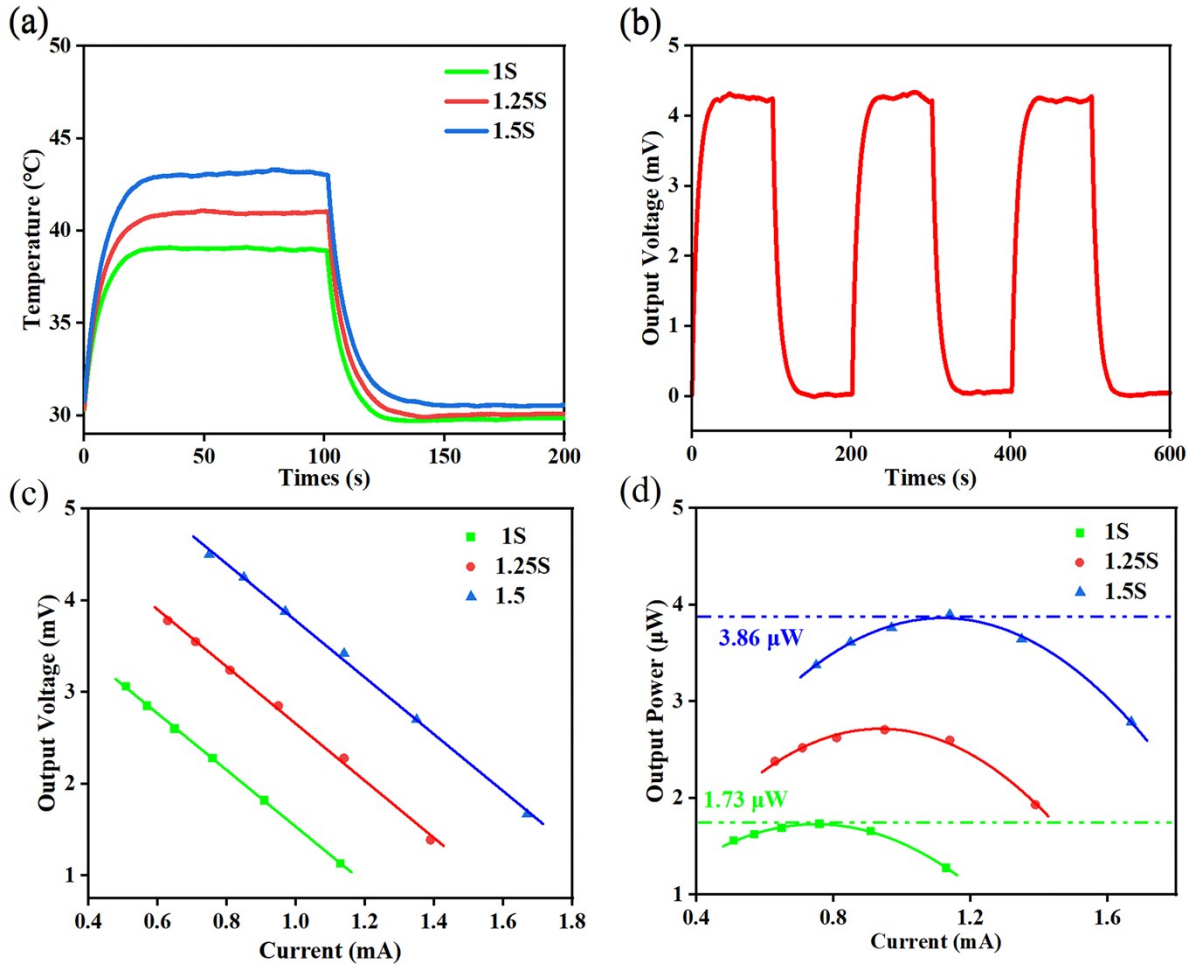

Figure S17. (a) Temperature changes of the 80Ag_2Se/20Nylon under different intensities of visible light irradiation. (b) The cyclic open-circuit voltage response of the PTEG under 1S visible light irradiation. (c) The output voltage and (d) power of the PTEG as a function of current at different radiation power of visible light.

Reference

1 X. Z. Jin, H. Li, Y. Wang, Z. Y. Yang, X. D. Qi, J. H. Yang and Y. Wang, *ACS Appl. Mater. Interfaces.*, 2022, **14**, 27083-27095.

2 D. L. Wen, X. Liu, J. F. Bao, G. K. Li, T. Feng, F. Zhang, D. Liu and X. S. Zhang, *ACS Appl. Mater. Interfaces.*, 2021, **13**, 21401-21410.

3 X. Z. Jin, X. D. Qi, Y. Wang, J. H. Yang, H. Li, Z. W. Zhou and Y. Wang, *ACS Appl. Mater. Interfaces.*, 2021, **13**, 8808-8822.

4 Z. Y. Yang, X. Z. Jin, C. H. Huang, Y. Z. Lei and Y. Wang, *ACS Appl. Mater. Interfaces.*, 2022, **14**, 33370-33382.

5 M. He, Y.-J. Lin, C.-M. Chiu, W. Yang, B. Zhang, D. Yun, Y. Xie and Z.-H. Lin, *Nano Energy*, 2018, **49**, 588-595.